Journal of Alloys and Compounds 782 (2019) 667–671

Contents lists available at ScienceDirect

Journal of Alloys and Compounds

journal homepage: http://www.elsevier.com/locate/jalcom

Beta titanium single crystal with bone-like elastic modulus and large crystallographic elastic anisotropy

Pan Wang [a, b, *], Mitsuharu Todai [a], Takayoshi Nakano [a, **]

[a] Division of Materials and Manufacturing Science, Graduate School of Engineering, Osaka University, 2-1 Yamadaoka, Suita, Osaka, 565-0871, Japan
[b] Singapore Institute of Manufacturing Technology, 73 Nanyang Drive, 637662, Singapore

ARTICLE INFO

Article history:
Received 8 November 2018
Received in revised form
16 December 2018
Accepted 18 December 2018
Available online 19 December 2018

Keywords:
Titanium alloys
Biomaterials
Elastic behavior
Anisotropy
Electrical resistivity

ABSTRACT

To develop single crystalline beta titanium implant as new hard tissue replacements for suppressing the stress shielding, we design a Ti-26.6Nb-6.7Al alloy (at. %) single crystal that exhibits large crystallographic elastic anisotropy and low Young's modulus. The anisotropy factor, *A*, reaches 3.42 that is the highest among all the reported values. The Young's modulus along <100> direction, E_{100}, is only 36 GPa that is similar to the Young's modulus of cortical bone. These results prove our proposed design strategy and provide a new path to design beta titanium single crystal with bone-like elastic modulus for implant to minimize stress shielding.

1. Introduction

Biocompatible low Young's modulus alloys should be developed to prevent the stress shielding that is bone degradation and absorption caused by the gap of Young's modulus between the replacement materials and natural human bone [1]. As an important category of Ti alloys, β-phase Ti alloys with body-centered cubic structures exhibiting low Young's modulus have been focused by many researchers as hard tissue replacements for both academic interesting and applications [1–7]. However, the Young's moduli of these polycrystalline are around 55–85 GPa and still higher than that of cortical bones, 20–40 GPa [1,6,7]. As one of the approaches, our group is trying to make single crystal β-Ti as hard tissue replacements by focusing on the control of crystal orientation and the development of the β-phase alloy with a low electron-atom (*e*/*a*) ratio [8,9]. It is suggested that the Young's modulus along <100> direction, E_{100}, in β-phase Ti single crystals with low *e*/*a* ratio is the lowest among all crystallographic orientations and the elastic anisotropy increase with decreasing the *e*/*a* ratio [5,8,9]. The *e*/*a* is the average number of valence electron per atom in the free atom configuration.

Recently, our group proposed a strategy to develop β-Ti alloys with extreme low moduli by reducing the *e*/*a* ratio in alloys and by suppressing the formation of the ω-phase at the same time, according to the examination of elastic properties of Ti-15Mo-5Zr-3Al alloy single crystal, an International Organization for Standardization (ISO) certified β-phase Ti alloy. Although the ω-phase is suppressed and the *e*/*a* ratio lows to 4.10 in this alloy, the E_{100}, ~44.4 GPa, is still higher than that of human cortical bones. This implies that there must be other factors influence the resultant Young's modulus. It is suggested that the Young's modulus of Ti-Nb alloys with low *e*/*a* ratio shows the lowest among Ti-Mo, Ti-V, Ti-Zr, Ti-Ta and Ti-W alloys [10]. Therefore, a selection of Ti-Nb base alloy is predictable to further decreasing the E_{100} in the newly designed alloy. Moreover, the appearance of lattice modulation is considered as an evidence of the lattice softening and low β-phase stability in some β Ti-Nb alloys that exhibit a low Young's modulus [4,11]. In this aspect, the present of lattice modulation is also an important clue for further decreasing the E_{100} in the newly designed alloy.

Based on the above description, therefore, four criteria are proposed as a complete design strategy for low Young's modulus and large crystallographic elastic anisotropy in β-Ti single crystal. They are (i) low Young's modulus base alloy system (for example,

* Corresponding author. Division of Materials and Manufacturing Science, Graduate School of Engineering, Osaka University, 2-1 Yamadaoka, Suita, Osaka, 565-0871, Japan.
** Corresponding author.
E-mail addresses: wangp@SIMTech.a-star.edu.sg (P. Wang), nakano@mat.eng.osaka-u.ac.jp (T. Nakano).

https://doi.org/10.1016/j.jallcom.2018.12.236

Ti-Nb alloy system), (ii) no precipitation of secondary phases, such as martensitic and/or ω-phase, (iii) low *e*/*a* ratio and (iv) formation of lattice modulation. Here, we designed a novel Ti-26.6Nb-6.7Al alloy single crystal that fulfilled the above four selection criteria. It is expected to be suitable for the development of single crystalline beta titanium implant as new hard tissue replacements for suppressing the stress shielding by achieving a drastic reduction in the Young's modulus.

2. Experimental procedure

The single crystal rod of the Ti-26.6Nb-6.7Al alloy was fabricated by an optical floating zone apparatus (Canon machinery: SCI-MDH-20020) at the crystal growth rate of 2.5 mm/h under a high purity argon gas flow from the ingots prepared by arc melting. The chemical composition of the single crystal, listed in Table 1, was analyzed by ICP-OES for Ti, Nb, Al, and IGA for the analysis for the elements O, N, and C. The *e*/*a* ratio for the Ti-26.6Nb-6.7Al single crystal is 4.19. Electrical resistivity was measured using a standard four probe method with a cooling and heating rate of 1 K/min [4]. XRD measurements were conducted at room temperature with Cu Kα radiation. The microstructure of the single crystal was observed by transmission electron microscopy (TEM; JEM-3010, JEOL) operated at 300 kV. The cubic specimens for elastic constants measurement were cut from the single crystal rods and were subsequently annealed at 1273 K for 1 h and then quenched into ice water. By the X-ray Laue back diffraction method analyzed, the surfaces of the specimen were parallel to the crystallographic {100} planes of the β-phase within an accuracy of 1°.

Table 1
Chemical compositions of Ti-26.6Nb-6.7Al single crystal and corresponding *e*/*a* ratio.

	Ti	Nb	Al	O	N	e/a
mass %	Bal.	42.4	3.1	0.072	0.013	
at.%	Bal.	26.6	6.7	0.263	0.054	4.19

The independent elastic stiffness components of cubic symmetry, c_{11}, c_{12}, and c_{44} were measured at room temperature by Rectangular Parallelepiped Resonance method. This method was developed in 1970s and has found successful applications recently [12,13]. In RPR method, the elastic constants (c_{ij}) that are determined from a series of resonance frequencies of mechanical vibration of the specimen. They are fitting parameters which gives optimal fit of theoretical resonance spectrum to experimentally measured one. Over 60 resonance peaks are used in our optimization process. To examine the anisotropy of the Young's modulus, the orientation dependence of Young's modulus in directions between the <100> and <011> directions was calculated by coordinate conversion of measured c_{ij}.

3. Results and discussion

The crystallographic characterization of Ti-26.6Nb-6.7Al single crystal rod was shown in Fig. 1a. Compared with polycrystalline Ti-26.6Nb-6.7Al alloy, only strong (200) peak of β phase was detected in the XRD profiles, confirming the orientation of the <100> crystal. Fig. 1b uncovers a temperature independence of electrical resistivity between 60 K and 125 K, signalizing a lattice modulation and low Young's modulus [3,4]. Fig. 1c manifests the electron

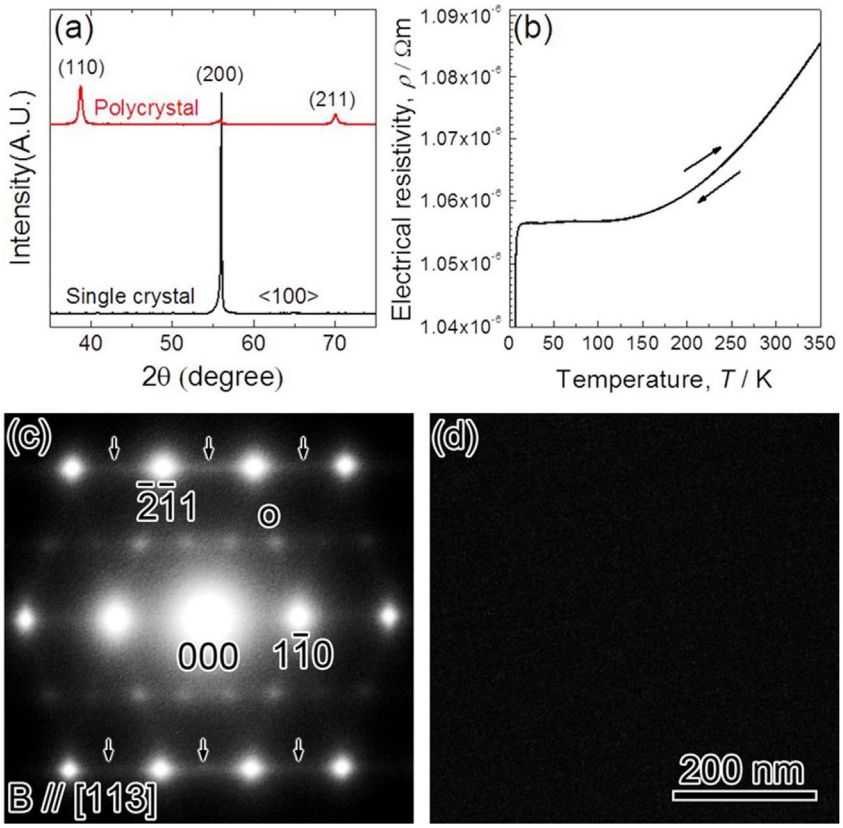

Fig. 1. (a) XRD profile of the <100> oriented crystal and polycrystal. (b) Temperature dependence of electrical resistivity of the single crystal. (c) Electron diffraction pattern and (d) dark field image of the single crystal in the beam direction [113]. The dark field image was observed using reflection denoted by a circle in Fig. 1(c) to show the possible presence of ω-phase.

diffraction pattern of Ti-26.6Nb-6.7Al single crystal in the beam direction [113]. Besides clearly fundamental spots derived from the β-phase with bcc lattice, we also observed the streaks along [110]* and diffuse satellites at $\boldsymbol{g}_\beta + 1/2[110]^*$ that was very weak and indicated by arrows in Fig. 1c, where the asterisk (*) implies orientation in a reciprocal lattice space and $\boldsymbol{g}_\beta$ is the β-phase reciprocal lattice vector. It is suggested that these are caused by the transverse lattice modulation [3,14,15]. The streaks along the <112>* direction and diffuse satellites at $\boldsymbol{g}_\beta + 1/3\langle\zeta\zeta 2\zeta\rangle^*$ and $\boldsymbol{g}_\beta + 2/3\langle\zeta\zeta 2\zeta\rangle^*$, which related ω-phase that always presented in various Ti-alloys with low β-phase stability [2,3,5,8,14], cannot be observed in the Ti-26.6Nb-6.7Al single crystal. This indicates that the prepared single crystal consisted almost entirely of the β-phase. Moreover, the dark field image (Fig. 1d) taken from the reflection denoted by a circle in Fig. 1c corresponding to the position of the reflection spot derived from the ω-phase indicates that no stable ω-phase was formed in the β-phase matrix. This is caused by the addition of Al and is in agreement with the previous studies [3,16].

The independent elastic stiffness components of cubic symmetry, c_{11}, c_{12}, and c_{44} were measured at room temperature by RPR method. From these c_{ij} components, the shear modulus $c' = (c_{11}-c_{12})/2$ for {110}<110> shear, bulk modulus $B = (c_{11} + 2c_{12})/3$ and anisotropy factor $A = c_{44}/c'$ were calculated and listed in Table 2.

Table 2
Elastic constants of Ti-26.6Nb-6.7Al single crystals: elastic stiffness of c_{11}, c_{12}, c_{44}, shear modulus, c', bulk modulus, B, and anisotropy factor, A.

Sample	c_{11}	c_{12}	c_{44}	c'	B	A
Ti-26.6Nb-6.7Al	144.24	119.12	42.96	12.56	127.49	3.42

Fig. 2 illustrates the calculated c', B, c_{44}, and A values, as a function of the e/a ratio, because the e/a ratio is believed to have a dominant influence on the elastic constants [17]. Those of reported binary β-Ti alloys, which consisted only of the β-phase (except for Ti– Cr alloy with an e/a ratio of 4.14 that consisted of the β-phase and ω-phase), were also presented for comparison. It is lucid that the c' (Fig. 2a) and B (Fig. 2b) values almost monotonically reduced with a decrease of the e/a ratio in both the present alloys and the binary β-Ti alloys consisting of only the β-phase. As a result, Ti-26.6Nb-6.7Al single crystal with the low e/a ratio and β-phase lattice modulation exhibited lowest c' among all of the binary β-Ti alloys. The c' value of Ti-26.6Nb-6.7Al single crystal (12.56 GPa) is also lower than that of the well-known Ti-Nb-Ta-Zr-(O) (13.5–14.5 GPa) [18] and Ti-15Mo-5Zr-3Al (15.9 GPa) [8] single crystals. Zener [19] has insisted that c' is a direct indicator of β-phase stability. A low c' corresponds to a low β-phase stability. Therefore, the β-phase stability of Ti-26.6Nb-6.7Al single crystal was quite low because of the examined c' value, which is in agreement with the previous result [3]. Independent of the e/a ratio, the c_{44} value of the alloys consisting of the β-phase is almost constant, except for the β + ω phase Ti–Cr alloy, as shown in Fig. 2c. The high c' and c_{44} values exhibited in the Ti–Cr alloy with an e/a ratio of 4.14 is caused by the presence of the ω-phase. The ω-phase has a higher elastic modulus than the β-phase in β-Ti alloys [25,26]. It is reported that the lattice is stabilized by the formation of ω-phase, resulting in the stiffening in c_{11} and c_{44} remarkable at low values of e/a in β-Ti alloy [27]. This is responsible to the local minimum of Young's modulus that appears at the composition just before the formation of the ω-phase [28]. In this study, the ω-phase formation was completely suppressed and single β-phase with

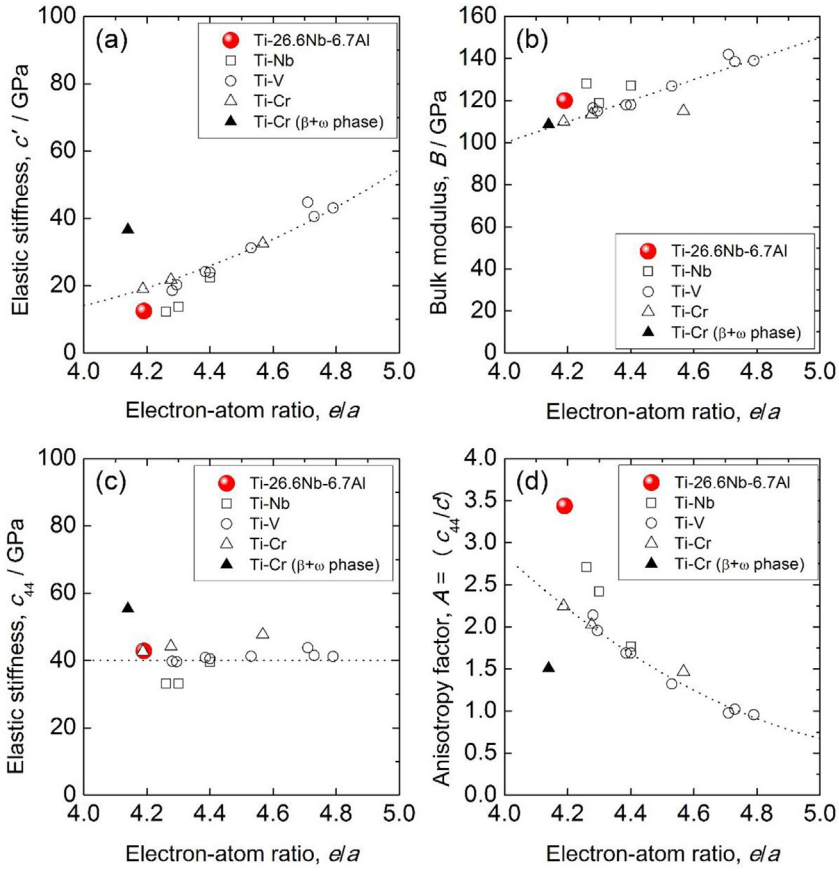

Fig. 2. (a) Comparison of elastic constants (a) c', (b) B, (c) c_{44}, and (d) anisotropy factor A between Ti-26.6Nb-6.7Al single crystals and binary β-Ti alloy (Ti-Nb [11,20,21], Ti-Cr [17], and Ti-V [22–24]) single crystals on the basis of e/a ratio.

lattice modulation was retained in the Ti-26.6Nb-6.7Al single crystal at room temperature and low temperature with the help of Al doping. On the other hand, e/a ratio also decreased by the addition of Al content [3], thus resulting in the peculiar low modulus.

Fig. 2d shows the comparison of the anisotropy factor A between the Ti-26.6Nb-6.7Al single crystal and the binary β-Ti alloys. A monotonous increase of the A values with a decrease in the e/a ratio was observed in the single β-phase alloys. Especially for Ti-Nb base alloys, the increase with a decrease in the e/a ratio is more remarkable than binary Ti-V and Ti-Cr alloys. As a result, the highest A value was observed in Ti-26.6Nb-6.7Al single crystal, owing to the lowest shear modulus c' of Ti-26.6Nb-6.7Al single crystal. It should be noticed that the anisotropy factor A (3.42) of current single crystal is also higher than that of the reported quaternary Ti-Nb base alloys (1.8–2.6) [9,18,29]. What's more, it is even higher than the 'strong crystallographic elastic anisotropy' alloy, Ti-15Mo-5Zr-3Al (2.9) [8], which has a low e/a ratio (4.10). This suggests that Ti-Nb base alloy is a suitable candidate for developing β-Ti alloys with large crystallographic elastic anisotropy. According to this trend, a further increase of A value could be reached by reasonable designing of new β-Ti-Nb base alloy with a lower e/a ratio. On the other hand, a formation of ω-phase decreases drastically the A value, which is observed in Ti–Cr alloy with an e/a ratio of 4.14. Therefore, it is proved that the suppression of the ω-phase and decrease of e/a ratio are crucial for large crystallographic elastic anisotropy [8].

To understand the advantage of using single crystals as biomedical implants, the ratio of E_{100} to the Young's modulus of polycrystals, E_H, was calculated. The E_{100} values were calculated from Ref. [9]

$$E_{100} = \frac{9}{1/B + 3/c'}. \quad (1)$$

and E_H was estimated from the Hill approximation [8]:

$$E_H = \frac{1}{2}\left\{\frac{9}{1/B + 15/(2c' + 3c_{44})} + \frac{5}{5/(9B) + 2/(3c') + 1/c_{44}}\right\} \quad (2)$$

using the independent elastic constants of the single crystals. Fig. 3 shows the maximum reduction in the Young's modulus by using the single crystal. The E_{100}/E_H ratio linearly decreases with a decrease of the e/a ratio in the single β-phase Ti-Nb base alloys. Therefore, a significant reduction in the Young's modulus, E_{100}/E_H of ~0.49, was achieved in the Ti-26.6Nb-6.7Al alloy.

To further lay bare the anisotropy of Young's modulus in the currently developed single crystal, the orientation dependence of Young's modulus in directions between the <100> and <011> directions was calculated by coordinate conversion of measured c_{ij} [8,9]. Fig. 4 shows the orientation dependence of Young's moduli in the Ti-26.6Nb-6.7Al, Ti-30Nb [11] and Ti-40Nb [21] single crystals in directions between <100> and <110>. The symbol θ denotes the angle from the <100> direction on the <110> zone axis. Young's modulus of these single crystals presented anisotropy as a function of θ. The crystallographic elastic anisotropy of Ti-26.6Nb-6.7Al ($e/a = 4.19$) single crystal displayed the highest and that of Ti-40Nb ($e/a = 4.40$) single crystal showed the lowest. It is suggested that the crystallographic elastic anisotropy of Ti-Nb base single crystal increases with decreasing of e/a ratio. Moreover, E_{100} is lower than Young's modulus along the <111> direction, E_{111}, where E_{100} and E_{111} are the lowest and highest among Young's moduli in all the directions, respectively. The E_{111}/E_{100} reaches 3.2. This is in agreement with the anisotropy in Young's modulus of Ti-Nb base alloys reported in previous studies [9,30]. The lowest Young's modulus

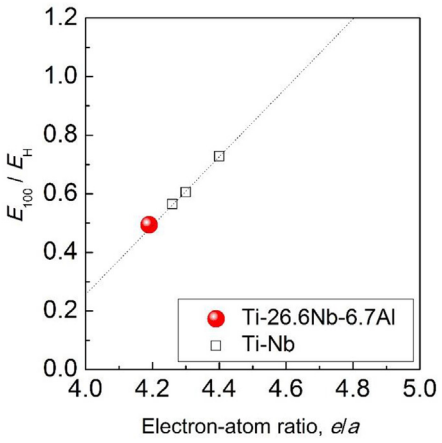

Fig. 3. E_{100}/E_H of Ti-26.6Nb-6.7Al single crystals and binary β-Ti-Nb [11,20,21] alloy single crystals as a function of e/a ratio. E_{100}/E_H is a ratio of Young's modulus of alloy single crystal along <100> direction, E_{100}, to the Young's modulus of alloys polycrystals, E_H.

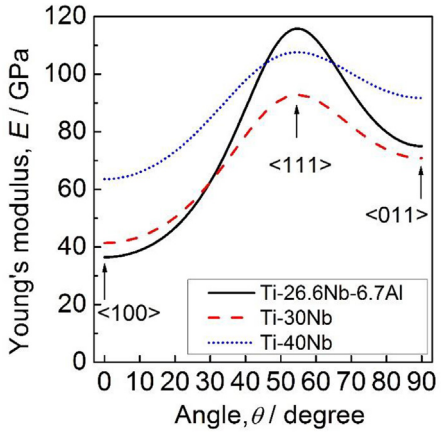

Fig. 4. Orientation dependence of Young's moduli of Ti-26.6Nb-6.7Al, Ti-30Nb [11] and Ti-40Nb [21] single crystals in directions between <1 0 0> and <1 1 0>, calculated by coordinate conversion of c_{ij}. θ is an angle from the <1 0 0> direction on the <1 1 0> zone axis.

E_{100} of the Ti-26.6Nb-6.7Al single crystal is relatively low at a value of only ~36 GPa because E_{100} is derived by low c' and B and is related to the decrease of the e/a ratio. This level is similar to the Young's modulus of cortical bone (20–40 GPa) and must effectively suppress the stress shielding when this single crystal was applied for biomedical implants. These results also mean that Ti-Nb base alloys exhibit a further reduction of the E_{100} modulus is possible by reasonable designing. Moreover, it should be noted that bone itself shows anisotropic behavior due to the preferential alignment of type I collagen and apatite crystal which are the dominant components of bone tissue. The apatite c-axis with a hexagonal crystal system strongly depends on the anatomical portion of bone, resulting in the anisotropic function; one-dimensional alignment in long bone and vertebral body bone, two-dimensional alignment in skull bone, etc. [31]. Thus, the designed anisotropic biomedical implant in this study is also similar to the anisotropic bone microstructure and its behavior.

4. Conclusions

In conclusion, the newly designed Ti-26.6Nb-6.7Al single crystal

displayed a low E_{100} (~36 GPa, which is similar to Young's modulus of cortical bone) and high E_{111}/E_{100} value (3.2). To our best knowledge, the Ti-26.6Nb-6.7Al single crystal exhibited the highest anisotropy, which is one of the most expected biomaterials to minimize stress shielding. While these results are interesting, more detailed investigation such as *in vitro* and *in vivo* experiments are required to further confirm the bone tissue compatibility of the newly developed single crystal metallic biomaterials. Nevertheless, these results open up a new avenue in terms of exploiting single crystal with low Young's modulus and large crystallographic elastic anisotropy as metallic biomaterials.

Acknowledgments

This work was supported by the Funding Program for Next Generation World-Leading Researchers from the Japan Society for the Promotion of Science (JSPS) and the Ministry of Education, Culture, Sports, Science and Technology (MEXT) of Japan and by the Grants-in-Aid for Scientific Research (S) from the Japan Society for Promotion of Science (JSPS).

References

[1] M. Geetha, A. Singh, R. Asokamani, A. Gogia, Prog. Mater. Sci. 54 (3) (2009) 397–425.
[2] J. Gao, Y. Huang, D. Guan, A.J. Knowles, L. Ma, D. Dye, W.M. Rainforth, Acta Mater. 152 (2018) 301–314.
[3] P. Wang, M. Todai, T. Nakano, J. Alloys Compd. 766 (2018) 511–516.
[4] P. Wang, M. Todai, T. Nakano, Mater. Trans. 54 (02) (2013) 156–160.
[5] M. Tane, S. Akita, T. Nakano, K. Hagihara, Y. Umakoshi, M. Niinomi, H. Mori, H. Nakajima, Acta Mater. 58 (20) (2010) 6790–6798.
[6] P. Wang, L. Wu, Y. Feng, J. Bai, B. Zhang, J. Song, S. Guan, Mater. Sci. Eng. C 72 (2017) 536–542.
[7] P. Wang, Y. Feng, F. Liu, L. Wu, S. Guan, Mater. Sci. Eng. C 51 (2015) 148–152.
[8] S.H. Lee, M. Todai, M. Tane, K. Hagihara, H. Nakajima, T. Nakano, J. Mech. Behav. Biomed. Mater. 14 (2012) 48–54.
[9] M. Tane, S. Akita, T. Nakano, K. Hagihara, Y. Umakoshi, M. Niinomi, H. Nakajima, Acta Mater. 56 (12) (2008) 2856–2863.
[10] H. Ikehata, N. Nagasako, T. Furuta, A. Fukumoto, K. Miwa, T. Saito, Phys. Rev. B 70 (17) (2004) 174113.
[11] R. Hermann, H. Hermann, M. Calin, B. Büchner, J. Eckert, Scr. Mater. 66 (3) (2012) 198–201.
[12] X. Ren, N. Miura, J. Zhang, K. Otsuka, K. Tanaka, M. Koiwa, T. Suzuki, Y.I. Chumlyakov, M. Asai, Mater. Sci. Eng. A 312 (1) (2001) 196–206.
[13] K. Tanaka, K. Okamoto, H. Inui, Y. Minonishi, M. Yamaguchi, M. Koiwa, Philos. Mag. A 73 (5) (1996) 1475–1488.
[14] M. Tahara, H.Y. Kim, T. Inamura, H. Hosoda, S. Miyazaki, Acta Mater. 59 (16) (2011) 6208–6218.
[15] M. Todai, T. Fukuda, T. Kakeshita, J. Alloys Compd. 577 (2013) S431–S434.
[16] J. Williams, B. Hickman, D. Leslie, Metall. Mater. Trans. B 2 (2) (1971) 477–484.
[17] E.S. Fisher, D. Dever, Acta Metall. 18 (2) (1970) 265–269.
[18] M. Tane, K. Hagihara, M. Ueda, T. Nakano, Y. Okuda, Acta Mater. 102 (2016) 373–384.
[19] C. Zener, Phys. Rev. 71 (12) (1947) 846–851.
[20] H. Jeong, Y. Yoo, Y. Lee, J. Park, J. Appl. Phys. 108 (6) (2010), 063515-063515-063516.
[21] C. Reid, J. Routbort, R. Maynard, J. Appl. Phys. 44 (1973) 1398.
[22] L.A. Ahlberg, O. Buck, N.E. Paton, Scr. Metall. 12 (11) (1978) 1051–1054.
[23] K. Katahara, M. Manghnani, E. Fisher, J. Phys. F Met. Phys. 9 (5) (1979) 773.
[24] E.S. Fisher, Physics of Solid Solution Strengthening, Plenum Press, New York, 1975.
[25] M. Tane, Y. Okuda, Y. Todaka, H. Ogi, A. Nagakubo, Acta Mater. 61 (20) (2013) 7543–7554.
[26] S. Sikka, Y. Vohra, R. Chidambaram, Prog. Mater. Sci. 27 (3) (1982) 245–310.
[27] E.W. Collings, The Physical Metallurgy of Titanium Alloys, ASM Series in Metal Processing, ASM International, Material Park, , Ohio, 1989.
[28] H. Matsumoto, S. Watanabe, N. Masahashi, S. Hanada, Metall. Mater. Trans. A 37 (11) (2006) 3239–3249.
[29] M. Tane, T. Nakano, S. Kuramoto, M. Niinomi, N. Takesue, H. Nakajima, Acta Mater. 61 (1) (2013) 139–150.
[30] Y. Zhang, S. Li, E. Obbard, H. Wang, S. Wang, Y. Hao, R. Yang, Acta Mater. 59 (8) (2011) 3081–3090.
[31] T. Nakano, K. Kaibara, Y. Tabata, N. Nagata, S. Enomoto, E. Marukawa, Y. Umakoshi, Bone 31 (4) (2002) 479–487.